Nuclear Instruments and Methods in Physics Research A 624 (2010) 321–329

Contents lists available at ScienceDirect

Nuclear Instruments and Methods in Physics Research A

journal homepage: www.elsevier.com/locate/nima

Development of the focal plane PNCCD camera system for the X-ray space telescope eROSITA

Norbert Meidinger [a,c,*], Robert Andritschke [a,c], Stefanie Ebermayer [a,c], Johannes Elbs [a,c], Olaf Hälker [a,c], Robert Hartmann [b,c], Sven Herrmann [a,c], Nils Kimmel [a,c], Gabriele Schächner [a,c], Florian Schopper [a,c], Heike Soltau [b,c], Lothar Strüder [a,c], Georg Weidenspointner [a,c]

[a] Max-Planck-Institut für extraterrestrische Physik, Giessenbachstrasse, 85748 Garching, Germany
[b] PNSensor GmbH, Römerstrasse 28, 80803 München, Germany
[c] MPI Halbleiterlabor, Otto-Hahn-Ring 6, 81739 München, Germany

ARTICLE INFO

Available online 23 March 2010

Keywords:
eROSITA
CAMEX
PNCCD
Spectroscopy
SRG
XMM-Newton
X-ray CCD detector

ABSTRACT

A so-called PNCCD, a special type of CCD, was developed twenty years ago as focal plane detector for the XMM-Newton X-ray astronomy mission of the European Space Agency ESA. Based on this detector concept and taking into account the experience of almost ten years of operation in space, a new X-ray CCD type was designed by the 'MPI semiconductor laboratory' for an upcoming X-ray space telescope, called eROSITA (extended Roentgen survey with an imaging telescope array). This space telescope will be equipped with seven X-ray mirror systems of Wolter-I type and seven CCD cameras, placed in their foci. The instrumentation permits the exploration of the X-ray universe in the energy band from 0.3 up to 10 keV by spectroscopic measurements with a time resolution of 50 ms for a full image comprising 384×384 pixels. Main scientific goals are an all-sky survey and investigation of the mysterious 'Dark Energy'. The eROSITA space telescope, which is developed under the responsibility of the 'Max-Planck-Institute for extraterrestrial physics', is a scientific payload on the new Russian satellite 'Spectrum-Roentgen-Gamma' (SRG). The mission is already approved by the responsible Russian and German space agencies. After launch in 2012 the destination of the satellite is Lagrange point L2. The planned observational program takes about seven years. We describe the design of the eROSITA camera system and present important test results achieved recently with the eROSITA prototype PNCCD detector. This includes a comparison of the eROSITA detector with the XMM-Newton detector.

1. Introduction

A new X-ray PNCCD detector was designed by the 'MPI Halbleiterlabor', the semiconductor laboratory of the Max-Planck-Institutes for physics and for extraterrestrial physics. It is based on the concept of the XMM-Newton PNCCD and considers the experience gained during ten years of its operation in space. The new detector was developed and tailored for the X-ray space telescope eROSITA, which is the acronym of 'extended Roentgen survey with an imaging telescope array'. It is an array of seven identical and parallel aligned telescopes. Each telescope consists of an X-ray mirror system of Wolter-I type and a PNCCD camera. A mirror system comprises 54 nested shells made of gold-coated nickel. It is designed to provide a point spread function (PSF) with a resolution of 15 arcsec half energy width (HEW) on-axis. The frame store PNCCD is accommodated in a distance of 1600 mm in the focal plane of the mirror system. Its field of view (FoV) has a diameter of 1.0°. The energy-dependent collecting area of the seven telescopes is, for example, 2400 cm^2 for X-rays of 1.5 keV energy and on-axis incidence.

This instrumentation permits the exploration of the X-ray universe in the energy band from 0.3 up to 10 keV by spectroscopic measurements. The PNCCD allows simultaneously highly resolved spectroscopy as well as imaging by means of a format of 384×384 pixels, which subdivide the 3 cm × 3 cm large CCD image area. The time resolution is chosen to 50 ms for a full image, resulting in a frame rate of 20 frames/s. In addition to very good energy, spatial and time resolution, the PNCCD provides high quantum efficiency for X-ray photon detection. The effective quantum efficiency of the detector, including the on-chip optical light filter necessary for operation in orbit, is at least 90% for X-ray photons in the energy range from 1 up to 11 keV.

2. The eROSITA mission

The eROSITA X-ray space telescope is motivated by various scientific goals [1,2]. The two most important topics are the

* Corresponding author. Tel.: +49 89 83940022; fax: +49 89 83940011
E-mail address: Norbert.Meidinger@hll.mpg.de (N. Meidinger).

0168-9002/$ - see front matter © 2010 Elsevier B.V. All rights reserved.
doi:10.1016/j.nima.2010.03.126

accomplishment of an all-sky survey and the measurement of 'Dark Energy'.

The first X-ray all-sky survey with an imaging telescope was carried out by the ROSAT satellite launched in 1990. Due to the use of a gas-filled proportional counter, the energy was limited to an energy band from 0.1 up to 2 keV. With eROSITA, the all-sky survey will be extended towards higher energies, actually up to about 10 keV. The highest energy is not limited by the solid-state detector but by the reflectivity of the mirrors because their collection area decreases steeply with increasing X-ray energy. The large collection area of the seven mirror systems and the high quantum efficiency of the detector over a broad energy band yield a higher sensitivity compared with ROSAT. For this reason, it is expected that eROSITA will detect significantly more black holes than ROSAT. Additionally, eROSITA will act as a pathfinder for future missions, such as the 'International X-ray Observatory' (IXO).

Observations of the cosmic microwave background and supernovae showed an accelerating expansion of the universe. This can be explained by 'Dark Energy', which dominates all other forms of energy but acts on scales comparable with the size of the universe. Thus, clusters of galaxies are excellently suited for this kind of precision cosmology. Since they are easily detectable in X-rays, eROSITA will focus on dark energy research. Simulations show that the detection of 100,000 clusters is possible. Such a number is needed for a precise measurement of the equation of state of the 'Dark Energy', and particularly for the measurement of 'baryonic acoustic oscillations' in the power density spectrum of galaxy clusters. These oscillations have been detected for the first time in 2005 and allow a model-independent determination of the cosmological parameters.

The eROSITA space telescope is developed under the responsibility of the 'Max-Planck-Institut for extraterrestrial physics' (MPE) in Germany. The instrument is part of the scientific payload on the new Russian satellite 'Spectrum-Roentgen-Gamma' (SRG). The mission is approved by the appropriate Russian and German space agencies, ROSKOSMOS and DLR. Launch of the satellite with a Soyuz-Fregat launch vehicle is planned for 2012 from Baikonur (Kazakhstan). Destination of the satellite will be the Lagrange point L2 in 1.5 million km distance from Earth. The planned observational program takes about seven years with four years dedicated to the all-sky survey.

3. PNCCD camera concept

The concept of the eROSITA PNCCDs is based on the very successful XMM-Newton PNCCD camera. In particular, its long-term stability is excellent: after 10 years in space on a highly eccentric orbit, the detector energy resolution showed almost no degradation. This is quantified by periodic measurements of the full-width at half-maximum (FWHM) value of the Mn-Kα line (5.9 keV) emitted by the on-board calibration source. The FWHM value changed only from 155 to 163 eV during 10 years of mission time.

3.1. Optimizations

Multiple optimizations of the PNCCD detector have been implemented for eROSITA, which are summarized in the following [3]. By redesign of the on-chip amplification structure and the CAMEX readout ASIC, the read noise was minimized to 2 electrons rms equivalent noise charge (ENC). For comparison, the XMM-Newton detector had a read noise of 5 electrons rms ENC.

The use of (1 0 0) silicon wafer instead of (1 1 1) oriented material and optimized doping profiles permit now excellent spectroscopy of low-energy X-ray lines, i.e. at energies far below 0.5 keV.

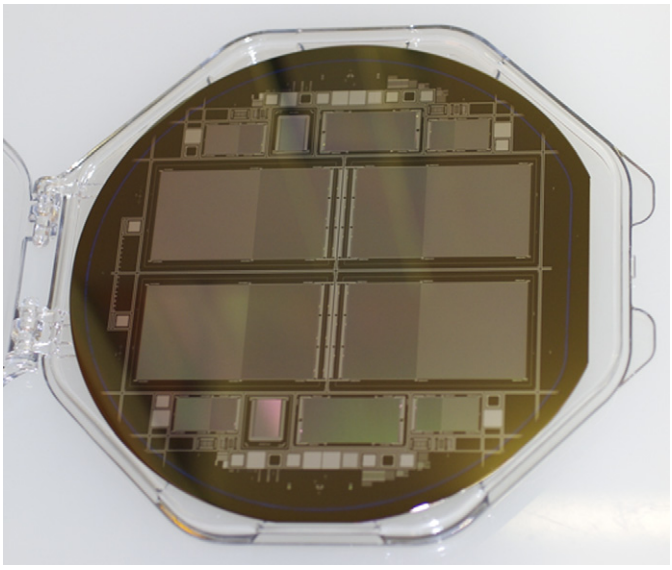

Fig. 1. CCD wafer containing four of the large-area eROSITA CCDs along with other detectors produced at MPI Halbleiterlabor.

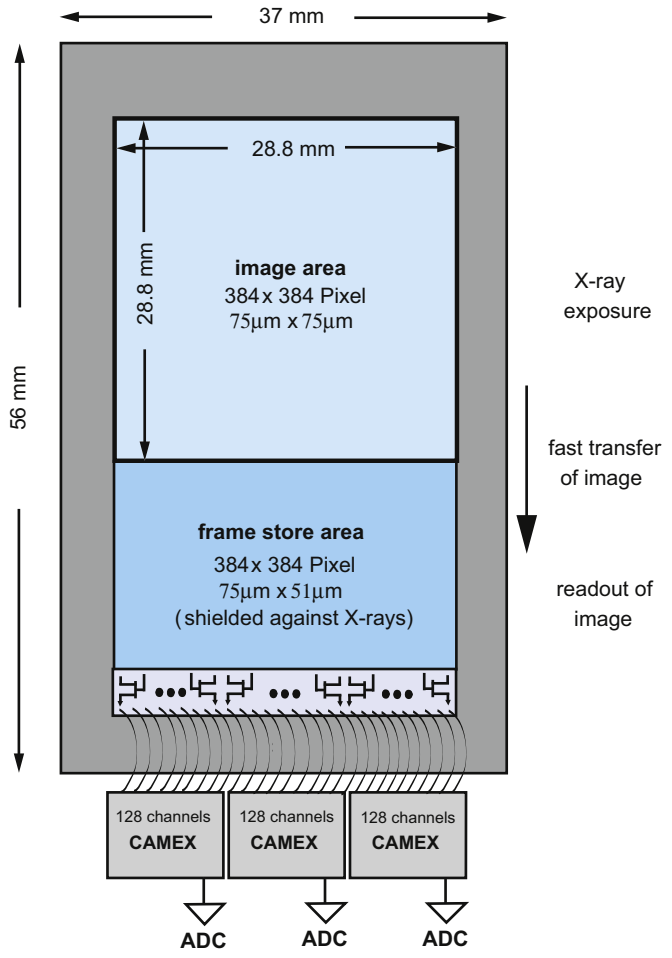

Fig. 2. Schematic drawing and geometry of the eROSITA detector. The PNCCD consists of the image and frame store area, and the on-chip electronics. The total image area is almost 3 cm × 3 cm large. The image is transferred during 115 µs from the image area to the frame store area. Each CCD channel is terminated by an anode, which is connected to the gate of a JFET. The source of each transistor is connected by a bond wire to a dedicated channel of the CAMEX analog signal processor. Signal transfer and processing are accomplished simultaneously for all 384 CCD channels. Finally, the 128 signals per CAMEX are multiplexed to its output buffer and fed into an ADC.

The interfering incidence of X-ray photons during transfer of the image to the anodes could be minimized by implementation of a frame store section on the CCD, which is shielded against X-rays. After accumulation of X-rays during the integration time, the image is rapidly transferred to the shielded frame store where the signals are readout. The occurrence of so-called 'out-of-time events' was thus lessened to a probability of only 0.2% in case of eROSITA. The previously, e.g. in case of the PNCCD camera on XMM-Newton, observed image smearing in transfer direction has thereby become negligible for the new PNCCDs.

The deposition of a light filter directly on the CCD chip as part of the device production process allows for a very compact camera. It simplifies the camera setup because the conventional external, large-area, self-supporting, ultra-thin and thus fragile light filter is no more necessary.

3.2. Concept and project specifications

The design of the eROSITA PNCCD was tailored to the specifications of the project. As a result it has a format of 384 rows and 384 channels in the image area with the same number of pixels in the frame store section (see Fig. 1). A pixel size of 75 μm × 75 μm was designed corresponding to an angular field of the telescope of 10 arcsec. The frame store pixels are shortened to 51 μm × 75 μm in order to keep the detector chip and its casing relatively small. The complete chip size including the anodes and on-chip electronics is 37 mm × 56 mm (see Fig. 2).

The X-rays photons are accumulated during an integration time of 50 ms in the image area. Then the image is transferred within 115 μs to the frame store and readout row by row while the next image is taken. The out-of-time event probability is therefore 0.23%. The readout time for the whole image takes about 10 ms. Afterwards the CAMEX is switched into standby mode to minimize heat dissipation. This is necessary to achieve a detector operating temperature of $\leq -80\,^{\circ}C$ for the seven cameras on the satellite. Apart from this thermal reason, the extended integration time provides time for on-board signal processing. This means in particular pixel wise offset and row wise common mode correction of the signals and then further signal selection by applying an upper and lower event threshold.

According to the concept of all PNCCDs of MPI Halbleiterlabor, each of the 384 CCD channels is terminated by an anode and the signals are amplified in an on-chip transistor (column parallel CCD) (see Fig. 2). Analog signal processing is done in the CAMEX ASIC, which provides 128 parallel channels for simultaneous signal processing of 128 CCD channels. Finally, all 128 signals are multiplexed after processing to one output buffer of the CAMEX

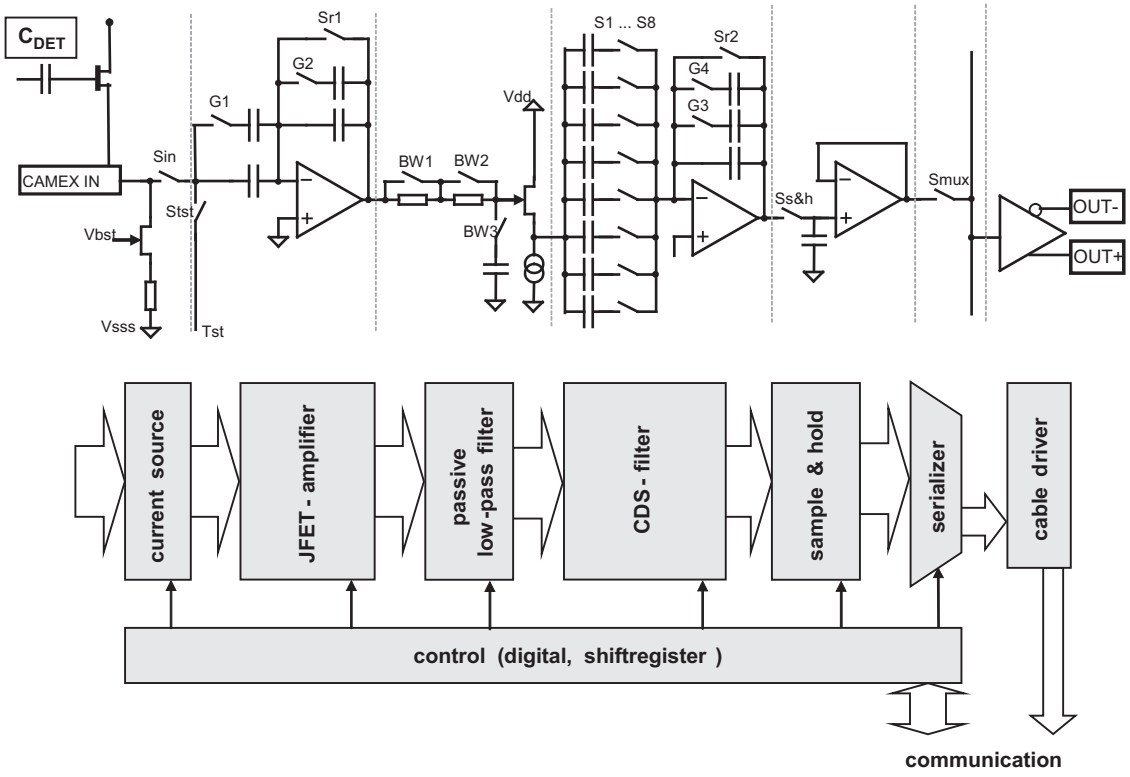

Fig. 3. Schematic diagram of one CAMEX analog signal processor channel (top) and the functional blocks (bottom).

Table 1
Components of the graded *Z* shield of the eROSITA detector.

layer	Element	Atomic number *Z*	Thickness (mm)	Fluorescence energy	Fluorescence yield K-shell vacancies (%)	Fluorescence yield L-shell vacancies (%)
1	Cu	29	30	0.9 keV, 8.0 keV, 8.9 keV	44	1.0
2	Al	13	1	1.5 keV	3.9	0.03
3	B_4C	5, 6	1	183 eV, 277 eV	0.2, 0.3	–
3	Be	4	1	109 eV	<0.2	–

and fed into a 14-bit ADC. Thus we need three CAMEX ASICs and ADCs for one eROSITA PNCCD detector.

3.3. CAMEX

The CAMEX (CMOS Analog Multiplexer) ASIC is designed for the readout of the PNCCD signals by the 'Ingenieurbuero Buttler' in Essen, Germany, in collaboration with the MPI Halbleiterlabor. Production of the 128-channel analog signal processor was done in a JFET-CMOS process technology by the 'Fraunhofer Institut fuer Mikroelektronik' in Duisburg, Germany. It is a 5 V process with 0.8 μm feature size. The CAMEX is equipped with a current source to bias the n-channel JFET of the PNCCD for operation in source follower mode. With a serial LVDS interface the internal registers are programmable. The signal filtering of the 128 channels is controlled by an on-chip digital sequencer with a width and depth of 16×64 bit. Low-noise performance is obtained by 8-fold correlated double sampling filtering of the voltage signals and an RC low pass filter, which limits the bandwidth (Fig. 3). By means of switching the three CAMEX processors in standby mode during about 80% of the time, we minimize the power dissipation and thus the active heat load to 0.7 W per cooled eROSITA detector in the focal plane.

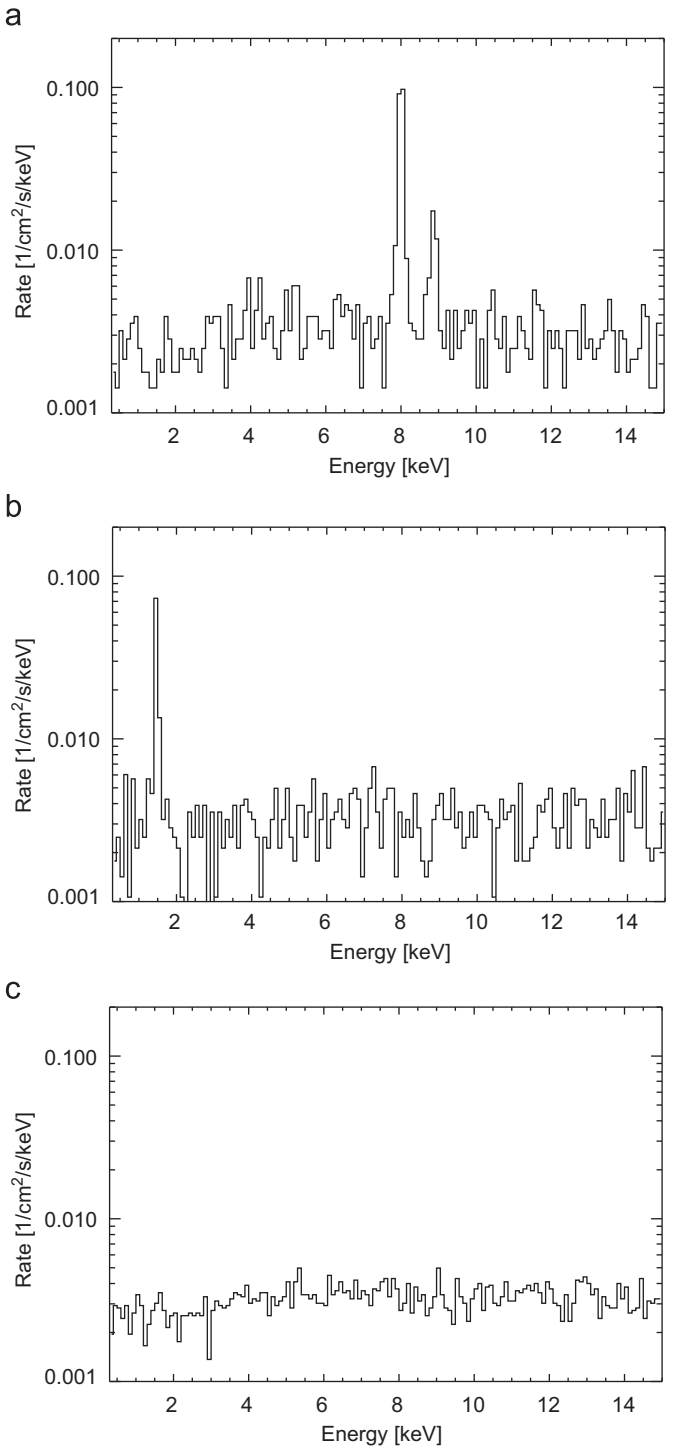

Fig. 4. (a–c) Simulation of the instrumental background spectrum of the eROSITA CCDs with SPENVIS and GEANT4-based Cosima. The charge signals of pixels, associated to the same event, are summed up as for real measurements. The figures, from top to bottom, show the background spectra resulting from a Cu shield, a Cu–Al shield and a Cu–Al–B_4C shield as described in the text.

3.4. Radiation environment

The recent decision to fly the eROSITA telescope not in a low-Earth orbit (600 km altitude, 30° inclination) but at Lagrange point L2 means a substantial change of the radiation environment. We studied the radiation environment in the new orbit for a mission time from 2012 to 2017 using SPENVIS (The Space Environment Information System), SRIM (The Stopping and Range of Ions in Matter) and GEANT4-based Cosima simulation software package [4], using a prototype version of an improved treatment of PIXE (particle induced X-ray emission) described by Pia et al. [5].

The eROSITA detectors will be shielded against protons by an approximately 30 mm thick copper shield except for the field of view. This aperture is shielded by the Wolter-I mirror system made of 54 tightly nested nickel shells in a coaxial and confocal configuration, which allows no straight unobstructed passage to the detector. 30 mm thick copper shields protons up to an energy of about 160 MeV. Only protons of higher energy can pass through the shielding and reach the detector. We calculated the remaining proton fluences for a simplified shielding, which consists of 30 mm copper all around the detector, i.e. including the entrance aperture.

Cosmic protons will result in a total fluence of $2 \times 10^8/\mathrm{cm}^2$ and solar protons in a total fluence of $1 \times 10^9/\mathrm{cm}^2$ on the detector. The associated non-ionizing energy loss (NIEL) is typically normalized to a proton energy of 10 MeV for the purpose of comparison. The equivalent 10 MeV proton fluence of cosmic and solar protons altogether on the eROSITA detector results in $5 \times 10^8/\mathrm{cm}^2$ for the first five years of the mission. We have planned irradiation tests with 10 MeV protons in the near future to study the damage effects for the eROSITA PNCCD and CAMEX ASICs.

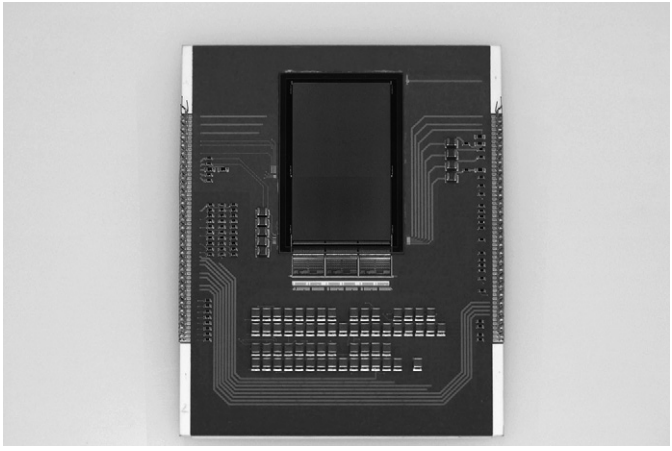

Fig. 5. Lab detector module for eROSITA CCD and CAMEX test.

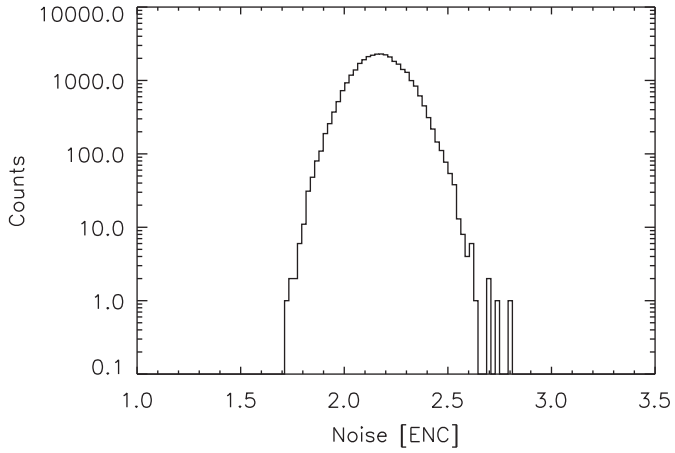

Fig. 6. Read noise spectrum measured with eROSITA CCD. The noise values of all 384×384 pixels are shown in the histogram.

Supply, control and data acquisition (DAQ) system electronics have to be equipped with sufficiently rad-hard components. Calculations with SPENVIS showed an ionization dose between 20 and 60 krad behind a typical minimum shielding thickness of 1 mm aluminum and during a mission time from 2012 to 2017 (in dependence on the various implemented models). Therefore, the baseline is to use 100 krad rad-hard components for eROSITA.

3.5. Instrument background

The instrument background of the XMM-Newton PNCCD camera is composed of strong fluorescence lines superposing the continuum contribution. This variety of fluorescence lines appearing in the observations of the X-ray sky is in consequence of the various chemical elements present in the vicinity of the CCD [7,8]. The dominant Al–K (1.5 keV) and Cu–K (8.0, 8.9 keV) fluorescence lines showed one to two orders of magnitude higher

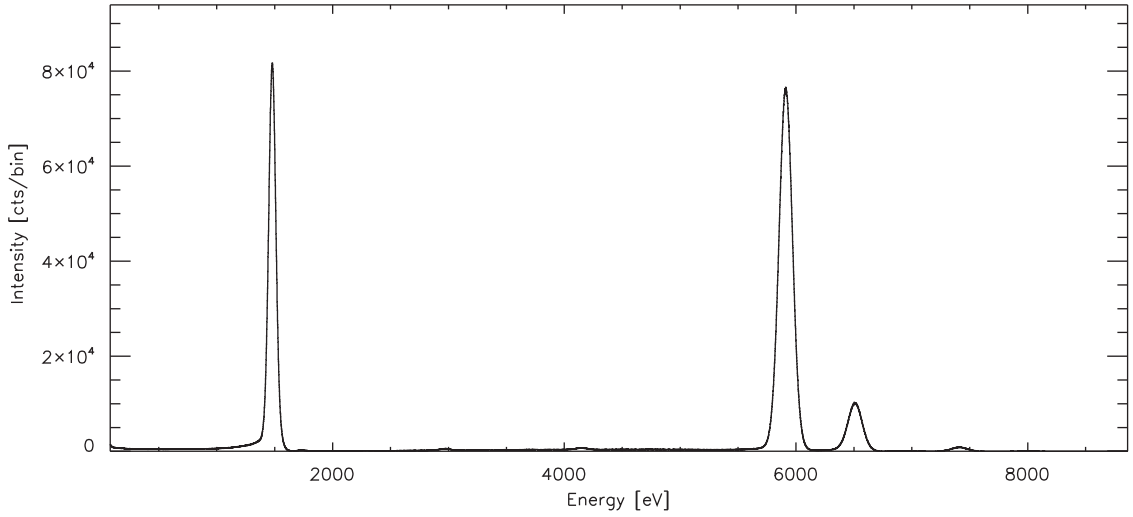

Fig. 7. Al–K (1.5 keV), Mn-Kα (5.9 keV) and Mn-Kβ (6.5 keV) spectra measured with an eROSITA PNCCD. Slightly above 4 keV we see indication of the Si-escape peak and at 7.4 keV we observe slight pileup of Mn-Kα and Al–K photons.

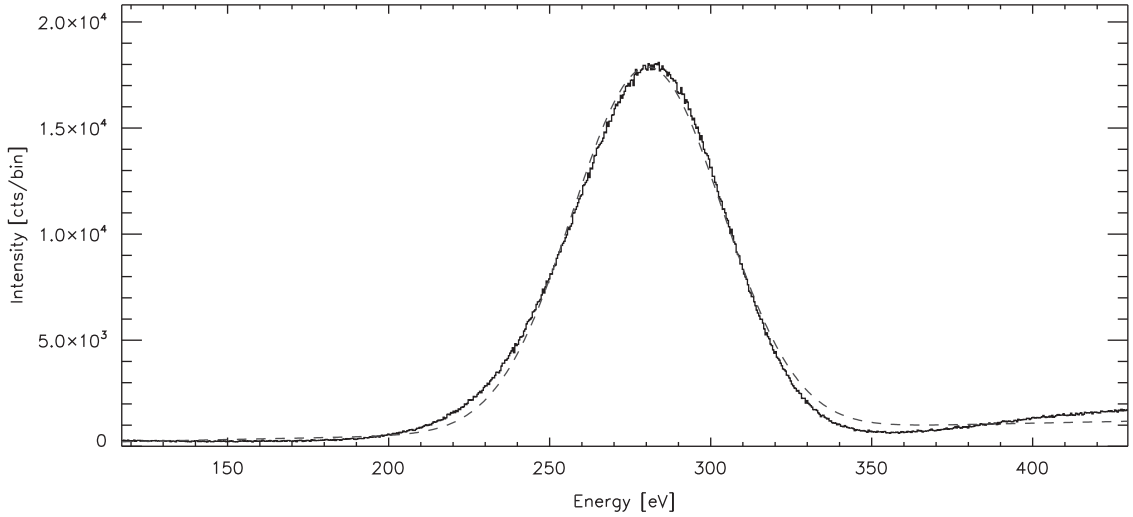

Fig. 8. C–K spectrum (277 eV) with Gaussian fit shown as dashed line.

rate compared with the continuum. Furthermore, several other less prominent fluorescence lines are visible in the spectra.

We plan for eROSITA a three-layer graded Z shield (Z, the atomic number) with appropriate layer thicknesses to suppress efficiently the fluorescence lines. The idea is to absorb fluorescence photons generated in an outer shell (with higher Z) within an inner shell (with lower Z). Thereby, energy and yield of fluorescence photons decrease layer for layer. The eROSITA graded Z shield consists essentially of 30 mm of copper as outer shell, which acts as proton shield, then 1 mm of aluminum and finally 1 mm of boroncarbide and beryllium, respectively, as innermost shell. Due to the very low Z material of the innermost shell, essentially Auger electrons (from non-radiative transitions) instead of fluorescence photons are generated (see fluorescence yields in Table 1 [6]). Auger electrons can easily be shielded due to the short range of electrons in matter compared to the attenuation length of X-rays of the same energy. A 10 keV electron has a range of 1.5 μm in silicon and for a 1 keV electron its range is <0.1 μm. The Auger electrons generated in carbon, boron and beryllium will thus be absorbed in the light filter of the photon entrance window (0.2 μm Al) and in the a few micron thick passivation layer on the opposite side of the PNCCD, respectively.

The remaining continuum of the instrument background is composed by two main contributions: (a) electrons from proton ionization of the material surrounding the detector and (b) recoil electrons of Compton scattered photons. These medium-energy electrons lose a portion of their energy in the material and the remaining energy is deposited in the CCD and cannot be distinguished from X-ray signals.

Primary highly energetic protons or electrons do not directly contribute to the continuum because their energy deposition in the CCD is, due to the large sensitive detector thickness of 450 μm, far above 15 keV (actually even above 100 keV). Thus they can be clearly identified and all signals belonging to the event pattern can be rejected.

A simulation of the instrumental background spectrum with GEANT4-based Cosima was carried out considering only cosmic protons, which show a more constant flux over time compared to solar protons. Solar protons appear more in flares but during a flare the observation with eROSITA will be stopped because of the very high background. In the simulation, we perform a pattern analysis of the events the same way as for our X-ray measurements. Only events with valid patterns of up to four pixels per event are counted and we sum up the energy of the associated pixels. The resulting background spectrum is shown in Fig. 4. The spectrum has a rather constant event rate of approximately 310^{-3}/cm^2 s keV in the energy range of interest between 0.3 and 15 keV. The figure shows strong Cu-Kα and Cu-Kβ fluorescence lines at 8.0 and 8.9 keV if only the Cu proton shield surrounds the CCD (Fig. 4a). The additional Al shield absorbs the Cu fluorescence lines but an Al fluorescence line at 1.5 keV is generated and detected in the CCD (Fig. 4b). The Cu–Al–B_4C shield accomplishes finally a background spectrum without interfering fluorescence lines (Fig. 4c). The continuum background spectrum obviously does not depend on the additional thin Al and B_4C layers.

4. Performance measurements

4.1. Energy resolution

The performance of eROSITA PNCCDs was tested in a laboratory test setup. Together with three CAMEX chips the CCD was mounted on a detector board (see Fig. 5) and operated under eROSITA relevant conditions, in particular with a frame rate of 20 frames/s and at a temperature of -80 °C.

We obtained in the measurements with several CCD detectors an average read noise in the range between 2.0 and 2.3 electrons rms. Fig. 6 shows a typical noise spectrum with a mean and median noise value of 2.17 electrons ENC. The noisiest pixel shows a value of 2.8 electrons ENC.

Table 2
Energy resolution of spectral lines measured with a large-format eROSITA PNCCD.

Line	Energy	FWHM (eV)
C–K	277 eV	53 (all), 52 (single)
Al–K	1.5 keV	74 (all), 72 (single)
Mn-Kα	5.9 keV	134 (all), 130 (single)

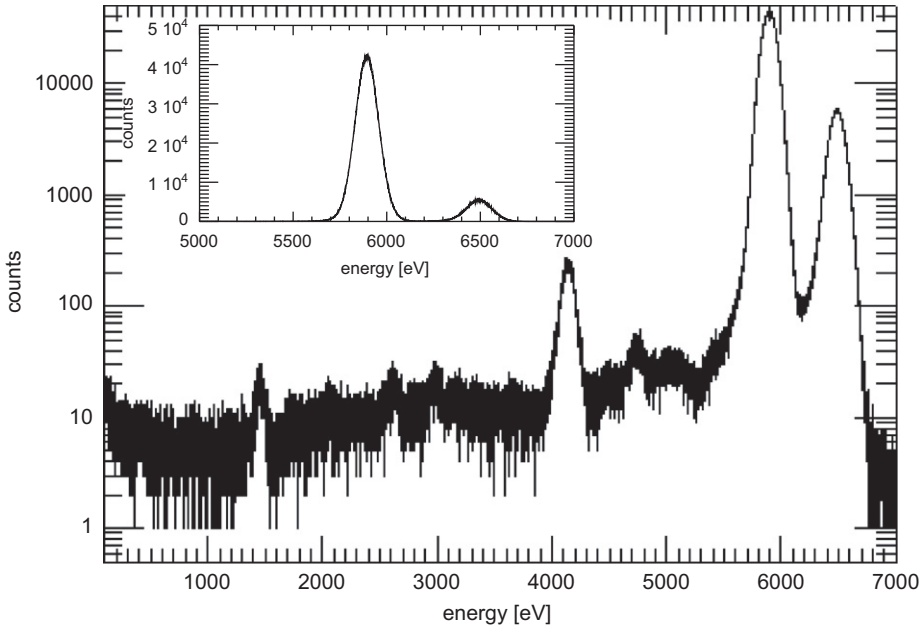

Fig. 9. Fe55 spectrum shown in logarithmic scale. Apart from the Mn-Kα and Mn-Kβ peaks, we observe the corresponding Si-escape peaks with 1.7 keV lower energy and the Al–K fluorescence line (1.5 keV) generated in the aluminum housing of the Fe55 source.

The spectra of a Fe55 source, an Al–K line and a C–K line are depicted in Figs. 7 and 8. The energy resolution expressed as FWHM of the lines is presented in Table 2. We list there separately the energy resolution obtained with 'all events' and just with 'single events' whose signal charge is collected in a single pixel resulting in a slightly better value. An excellent peak-to-valley ratio of 7500:1 was measured with these PNCCDs, which are already equipped with a light filter on the photon entrance window (Fig. 9).

4.2. Intensity maps

Fig. 10 shows a flat field measurement with six million Al–K (1.5 keV) X-ray photons accumulated in single photon counting mode. For this purpose we took 10,000 single PNCCD frames. The average total number of X-ray photons is about 41 per pixel. Most important is the absence of bright or not-transferring pixels, which can appear particularly in large-format PNCCDs. Another intensity map is presented in Fig. 11 where the Al–K X-rays illuminate the PNCCD through a mask with various structures to point out the imaging features of the detector. Finally, minimum ionizing particle (MIP) tracks were measured in dark field (without X-rays) and depicted in Fig. 12. We selected MIPs with

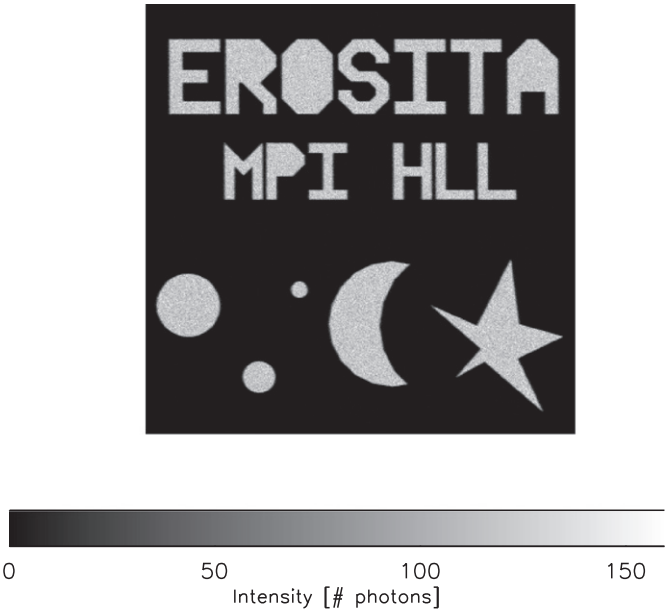

Fig. 11. X-ray illumination of the PNCCD through a mask.

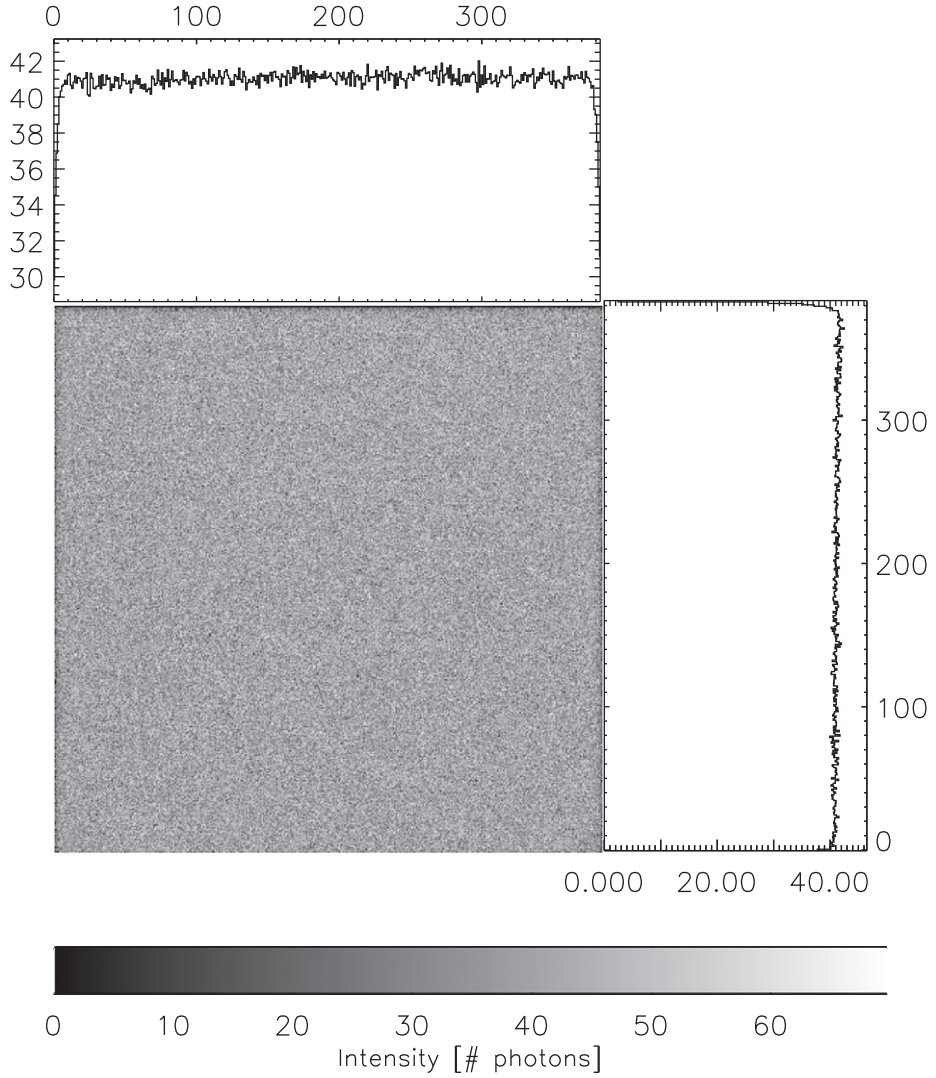

Fig. 10. X-ray intensity map of eROSITA PNCCD in flat field measurement.

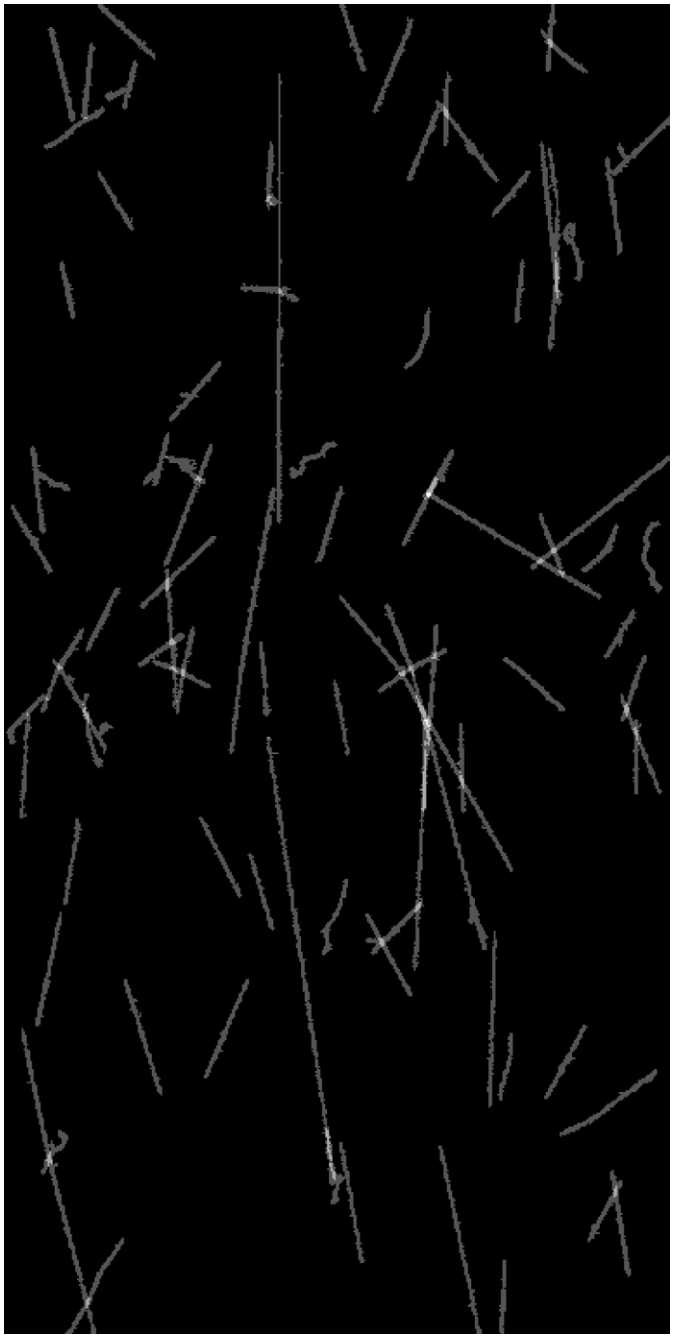

Fig. 12. Selected prominent MIP tracks measured in dark field with an eROSITA PNCCD detector in full frame mode (384 × 768 pixels).

very long tracks and observe clearly the crossings of tracks by the higher contrast.

4.3. Quantum efficiency

The ultra-thin and unstructured photon entrance window of the back-illuminated PNCCD in combination with full depletion of 450 μm detector thickness results in high quantum efficiency of at least 90% over the entire energy band from 0.3 up to 11 keV. The application of the detector in space requires a light filter to avoid interference of the X-ray signals with electrons generated by optical light. This is realized for eROSITA by a 200 nm thick Al layer deposited together with a thin Si_3N_4 and SiO_2 layer on the photon

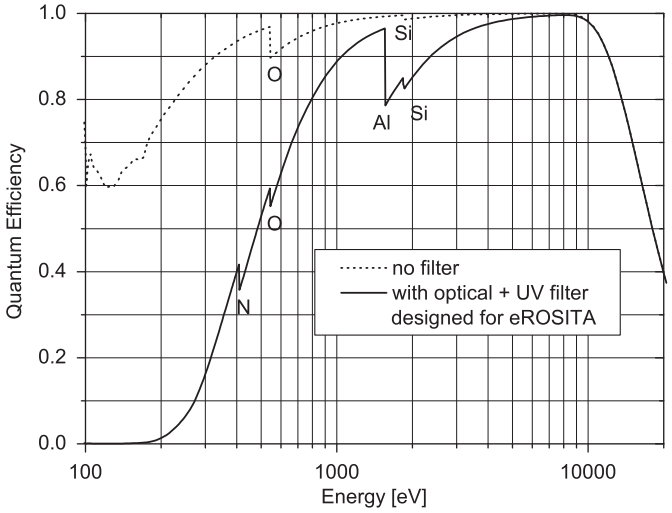

Fig. 13. Quantum efficiency of the PNCCD with and without deposited light filter. The curves are calculated, but in case without filter, the values are already confirmed by measurements.

entrance window. Transmission of optical light is suppressed by five to six orders of magnitude due to this filter. The trade-off is a reduced quantum efficiency for low-energy X-ray photons. The corresponding quantum efficiencies of the detector with and without light filter can be seen in Fig. 13. The most prominent absorption edge is that of the aluminum filter layer but the quantum efficiency is still 79% there. In contrast to other X-ray missions, the on-chip light filter contains no carbon and thus no carbon absorption edge appears, which would strongly decrease the detection efficiency for energies above 277 eV. With the eROSITA detector, quantum efficiencies of 16%, 40% and 53% are achieved at the very low photon energies of 0.30, 0.40 and 0.50 keV.

5. Outlook

The development of the focal plane detector for eROSITA has now reached an important phase. The first flight-type PNCCDs have been produced and tested together with the associated CAMEX analog signal processors. The detector boards used for the tests have similar design as those which are presently developed for the flight cameras. The experimental results have verified the detector concept and promise excellent performance for the eROSITA space telescope. Nevertheless, important tests such as radiation hardness measurements as well as final integration, test and qualification of the seven flight cameras have to be carried out with great accuracy before the eROSITA PNCCD instrument is ready for the flight to Lagrange point L2.

Acknowledgments

The authors are grateful to all colleagues who supported the detector development, fabrication and tests, in particular the eROSITA team, the staff of the MPI Halbleiterlabor, the Max-Planck-Institut für extraterrestrische Physik and the Max-Planck-Institut für Physik. This work was also supported by the DLR and the Heidenhain foundation.

References

[1] P. Predehl, G. Hasinger, H. Böhringer, et al., Proc. SPIE 6686 (2007) 17.
[2] P. Predehl, G. Hasinger, H. Böhringer, et al., Proc. SPIE 6266 (2006) P-1.

[3] N. Meidinger, R. Andritschke, O. Hälker, et al., Nucl. Instr. and Meth. A 568 (2006) 141.
[4] A. Zoglauer, R. Andritschke, S.E. Boggs, et al., Proc. SPIE 7011 (2008) 3F-1.
[5] M.G. Pia, G. Weidenspointner, M. Augelli, et al., IEEE Trans. Nucl. Sci. 56 (6) (2009) 3614.
[6] R.B. Firestone, Table of Isotopes, 8th ed., John Wiley & Sons, New York, 1996.
[7] M. Freyberg, U.G. Briel, K. Dennerl et al., Technical Note, EPIC_CAL-TN-0068-0-1.
[8] L. Strüder, U. Briel, K. Dennerl, et al., Astron. Astrophys. 365 (2001) L18.